SARTORIUS

Application Note

September 2022

Keywords or phrases:
Cell Migration, Scratch Wound, Label-Free Analysis, Wound Healing, Cell Movement, Cell Cycle

Dynamic Quantification of Cell Migration in Real Time

Amber Ward, Jasmine Trigg, Kalpana Barnes, Gillian Lovell, and Tim Dale
Sartorius UK Ltd., Units 2 & 3 The Quadrant, Newark Close, Royston Hertfordshire SG8 5HL UK

Correspondence
Email: AskAScientist@sartorius.com

Introduction

Cell migration is a multistep process that plays a fundamental role during essential physiological processes, such as immune cell migration and embryonic development, as well as pathological conditions, such as tumor metastasis. Cell migration is instigated by environmental stimuli initiating the rearrangement of actin filaments and microtubules at the leading edge.[1] The leading edge guides the cell across the substrate by forming tight integrin-based focal adhesions.[2] Membrane retraction at the lagging cell edge finishes the cycle, which is then repeated in rapid succession. It is the summation of these processes that produces the kinetic changes associated with cell migration.

Tumor metastasis is one of the key hallmarks of cancer and is intrinsically linked to the dysregulation of pathways associated with cell migration. Metastasis is the formation of a secondary tumor site caused by malignant cells detaching from their basement membrane and migrating via the vascular or lymphatic circulatory systems to a new site.[3] Thus, cell migration, along with other processes including cell invasion, underpin both the formation and survival of tumors. Furthering our understanding of these processes is important in limiting tumor progression and survival in future therapies.

Standard approaches to studying cell migration, such as creating a wound using a narrow object, can be time-consuming, inconsistent and rely heavily on end-point analyses. Live-cell analysis methods have been developed that provide a solution to robustly measure cell migration in real time.

Find out more: www.sartorius.com/incucyte

Assay Principle

In this application note, we describe the value of the Incucyte® Scratch Wound Cell Migration Assay, which utilizes the Incucyte® Live-Cell Analysis System in combination with the Incucyte® Scratch Wound Analysis Software Module for automated image-based measurements of cell migration *in vitro*. This flexible assay can be performed accurately across a range of cell lines and compounds. Here, we exemplify the ability to visualize and quantify cell migration kinetics in a 96-well format.

Materials and Methods

The Incucyte® Scratch Wound Assay involves a simple protocol that utilizes the Incucyte® 96-Well Woundmaker Tool to simultaneously create precise, uniform wounds in cell monolayers cultured on Incucyte® Imagelock 96-well Plates (Figure 1). The use of Incucyte® Imagelock Plates ensures that the wounds are automatically located and registered by integrated Incucyte® software.

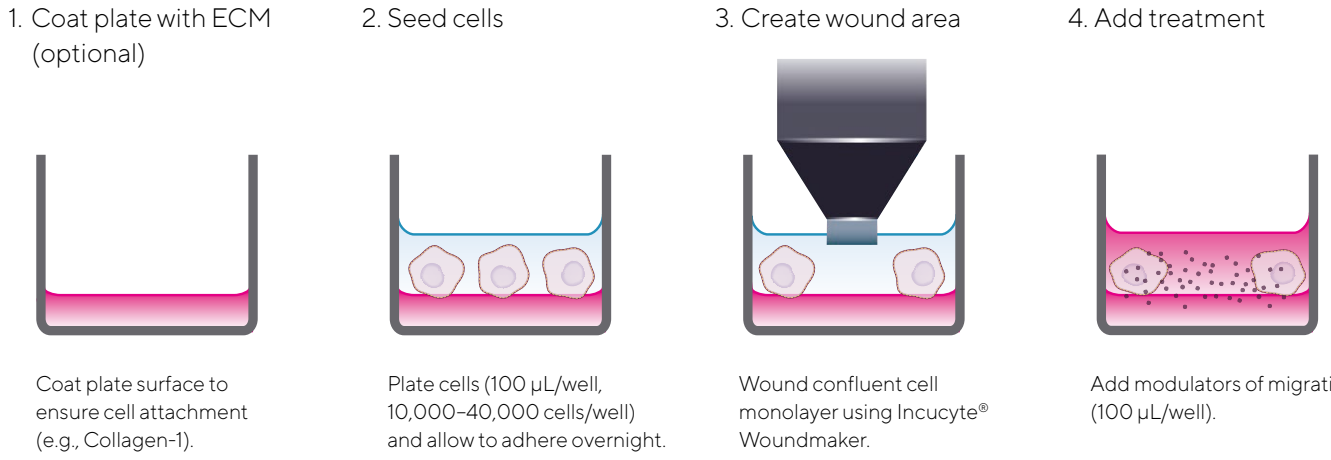

Figure 1: Quick Guide of Incucyte® Scratch Wound Assay Protocol. The simple protocol utilizes the Incucyte® Woundmaker and the Incucyte® Live-Cell Analysis System for image-based measurements of cell migration in real time.

1. Wells were either left uncoated or had a layer of biomatrix applied to ensure the tight adherence of cells to the well.
2. Cells of interest are seeded into an Incucyte® Imagelock Plate and incubated at 37 °C with 5% CO_2 overnight.
3. Optional: To ensure true detection of migration, cells once confluent can be pre-treated with an anti-proliferative agent such as mitomycin C (MMC). The concentration and pre-incubation time will need to be optimized for each cell type.
4. Confluent cell monolayer is wounded using the Incucyte® 96-Well Woundmaker Tool.
5. After washing, media containing treatments are added (100 µL/well at 1X final assay concentration (FAC)).

Quantification of Cell Migration

The Incucyte® Scratch Wound Analysis Software Module enables automated quantification of cell migration via label-free or dual fluorescence readouts in real time. We examined two proteins within the PI3K-Akt pathway—phosphoinositide-3-kinase (PI3K) and its antagonist phosphatase and tensin homolog (PTEN)—both of which regulate cell migration.[4] To assess their effects, we used HeLa wild type (WT) cells and two HeLa knockout cell lines of either PI3K (abcam, ab257029) or PTEN (abcam, ab255419). Shown are phase images of HeLa WT cells over 24 hours, with segmentation masks denoting the initial scratch (blue) and wound closure over time (yellow) (Figure 2A). Cell migration can be quantified using the Relative Wound Density (RWD) metric, calculated by comparing the cell density outside the wound to the cell density inside the wound. Data revealed that the knockout cell lines have an impeded migration rate, with 60% for WT, 40% for PI3K knockout and 38% for PTEN knockout at 48 hours (Figure 2B). Interestingly, full wound closure was not observed across all cell lines. This data highlights how this assay enables cell line comparison and the study of proteins implicated in migration signaling pathways.

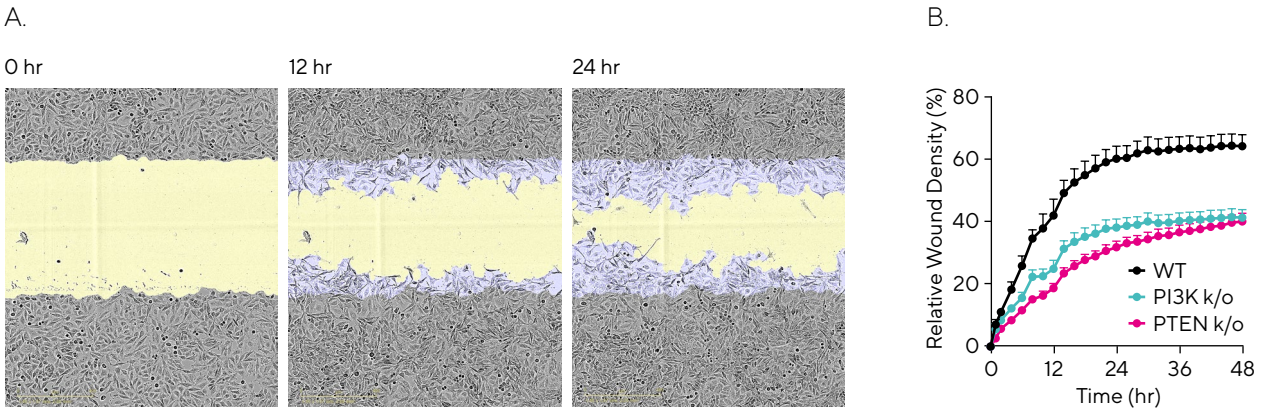

Figure 2: Quantifying Migration Profiles of HeLa WT and Knockout Cell Lines. HeLa WT, HeLa PI3K knockout and HeLa PTEN knockout cell lines were seeded into an Incucyte® Imagelock Plate (30,000 cells/well) and allowed to adhere overnight. Precise, reproducible wounds were created using the Incucyte® Woundmaker Tool and phase-contrast images were acquired every 2 hours using the Incucyte® Live-Cell Analysis System. (A) Time-lapse phase images shown migration for HeLa WT cells over 24 hours, with segmentation masks shown for initial scratch (blue) and wound closure over time (yellow). (B) Kinetic quantification revealed differential migration rates for WT vs knockout cells, which plateaued by 48 hours for all cell lines. Data shown as mean ± SEM, n = 12 replicates.

Optimization of Migration Assay Conditions

One consideration when conducting cell migration assays is that the closure of the wound may be partially driven by proliferation. Mitomycin C (MMC) is an anti-proliferative compound commonly used to control for proliferation in scratch wound assays.[5,6,7] To investigate this, MDA-MB-231 and BxPC3 cells were wounded after incubation with 50 µM MMC and phase images acquired (Figure 3A). MDA-MB-231 showed a faster migration rate compared to BxPC3 cells, with RWD of 95.3% compared to 66.9% for vehicle respectively by 24 hours (Figure 3B). MMC had no effect on the migration rate in MDA-MB-231 cells, indicating wound closure is primarily driven by migration. The slower migratory BxPC3 cells have an increased window for proliferation to occur. MMC pre-incubation attenuated migration compared to vehicle, which suggests that proliferation contributes to wound closure in this cell line. This highlights how anti-proliferative compounds can facilitate standardization of results for certain cell types.

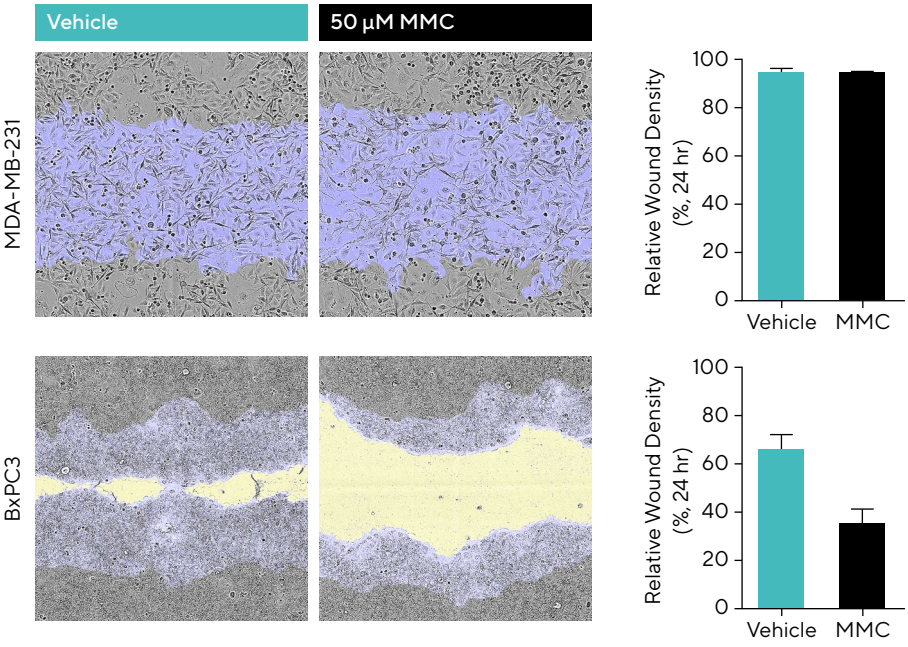

Figure 3: Anti-Proliferative Effects of Mitomycin C (MMC) During Cell Migration. MDA-MB-231 and BxPC3 cells were seeded (30,000 cells/well and 50,000 cells/well, respectively) and, once a monolayer had formed, pre-treated with 50 µM MMC for 4 hours. Cells were wounded, washed and migration was monitored using the Incucyte® Live-Cell Analysis System. (A) Phase images at 24 hours show reduced wound closure in the presence of MMC in BxPC3 but not MDA-MB-231 cells compared to vehicle. Segmentation masks shown for initial wound mask (blue) and wound closure over time (yellow). (B) Bar graphs indicate that for MMC, BxPC3 showed attenuated migration compared to vehicle, while MDA-MB-231 cells showed no reduction indicating wound closure is driven by migration. Data shown as mean ± SEM, n = 6–8 replicates.

Fetal bovine serum (FBS) is a universal component of cell culture media and contains factors crucial for cell attachment, growth, and proliferation.[8] We investigated T98G cell migration when exposed to FBS (0–10%) (Figure 4). In the absence of serum (0% FBS), cells displayed RWD of 63.6% after 24 hours, but increasing the percentage of serum correlated with an increase in migration rate, up to a maximal RWD of 92.6% in 10% FBS (Figure 4A). Furthermore, images indicate changes in cell morphology, with an extensive, elongated phenotype observed for 0% compared to 10% FBS (Figure 4B).

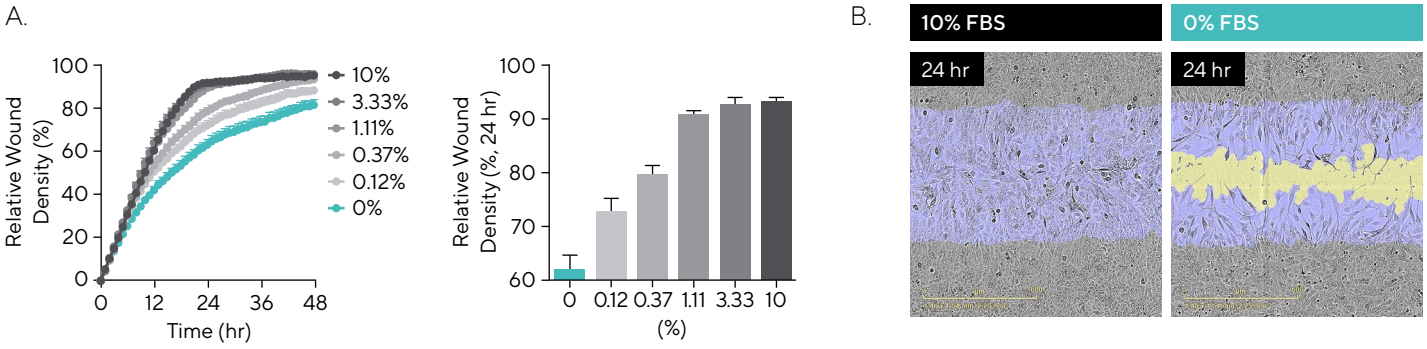

Figure 4: Cell Migration in the Presence of Serum. T98G glioblastoma cells were seeded onto PDL pre-coated Incucyte® Imagelock Plates (30,000 cells/well) and wounded after 24 hours. Media was added containing fetal bovine serum (FBS; 0–10%). (A) Time-course shows the rate slows with decreased serum, while comparison at the 24-hour time-point shows a linear increase in RWD between 0% and 10%. (B) Phase images at 24 hours post-scratch show reduced migration in the absence of serum, with segmentation masks shown for initial wound mask (blue) and wound closure over time (yellow). Images also allow for qualitative morphological assessment and indicate changes in cell morphology with a more elongated phenotype for 0% FBS. Data shown as mean ± SEM, n = 3 replicates.

Pharmacological Assessment of Inhibitors of Cell Migration

Scratch wound assays are commonly used to pharmacologically assess compounds of interest. Two highly migratory cell types, HT-1080 and MDA-MB-231, were wounded and exposed to PP242 (mTOR inhibitor) and cytochalasin D (inhibits actin polymerization). The microplate graph shows the RWD of these compounds over a 72-hour period, highlighting the consistency between replicates (Figure 5A). Cytochalasin D exerted concentration-dependent inhibition for both cell lines, with increased potency for HT-1080 cells. PP242 exhibited concentration-dependent inhibition in MDA-MB-231 cells and partial inhibition in HT-1080 cells (Figure 5B).

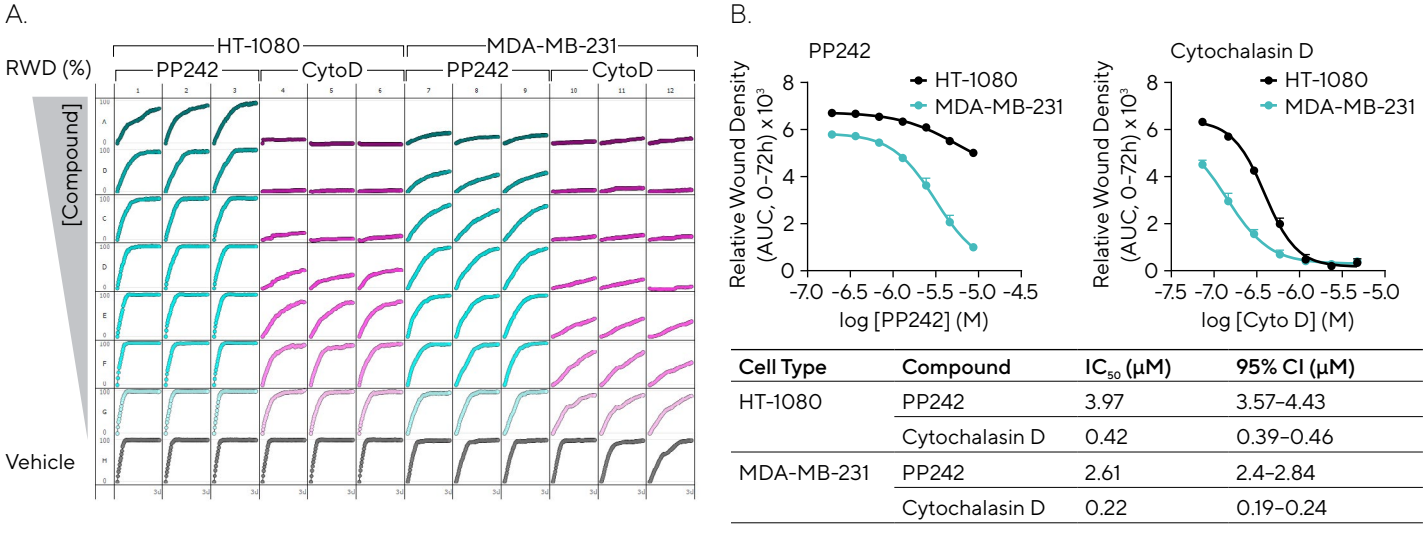

Cell Type	Compound	IC_{50} (µM)	95% CI (µM)
HT-1080	PP242	3.97	3.57–4.43
	Cytochalasin D	0.42	0.39–0.46
MDA-MB-231	PP242	2.61	2.4–2.84
	Cytochalasin D	0.22	0.19–0.24

Figure 5: Pharmacological Assessment of Inhibitory Compounds in Cancer Cell Lines. HT-1080 and MDA-MB-231 cells (30,000 cells/well) were wounded and treated with PP242 (mTOR inhibitor) and cytochalasin D (actin polymerization inhibitor). (A) 96-well microplate graph showing relative wound density (RWD) over 72 hours enables visualization of cell migration in the presence of inhibitors. (B) Concentration response curves indicate the efficacy of each compound (AUC, 0–72h) in both cell types with IC_{50} values and confidence interval (CI) shown (Table). Data shown as mean ± SEM, n = 3 replicates.

HT-1080 fibrosarcoma cells and 3T3 murine embryonic fibroblasts were utilized to evaluate three PI3K inhibitors.[9] Time-courses show varying migratory kinetic profiles for different compounds and indicate PI3K inhibitors are more potent to 3T3 than HT-1080 cells (Figure 6). HT-1080 cells have an activated n-RAS oncogene which, through sustained signaling, could confer resistance to inhibitors of downstream pathways, such as PI3K.[10] Also, in HT-1080 cells the selective inhibitor Wortmannin shows greater inhibition of migration compared to non-selective inhibitors. Overall, these data highlight how this assay enables robust profiling of compound effects.

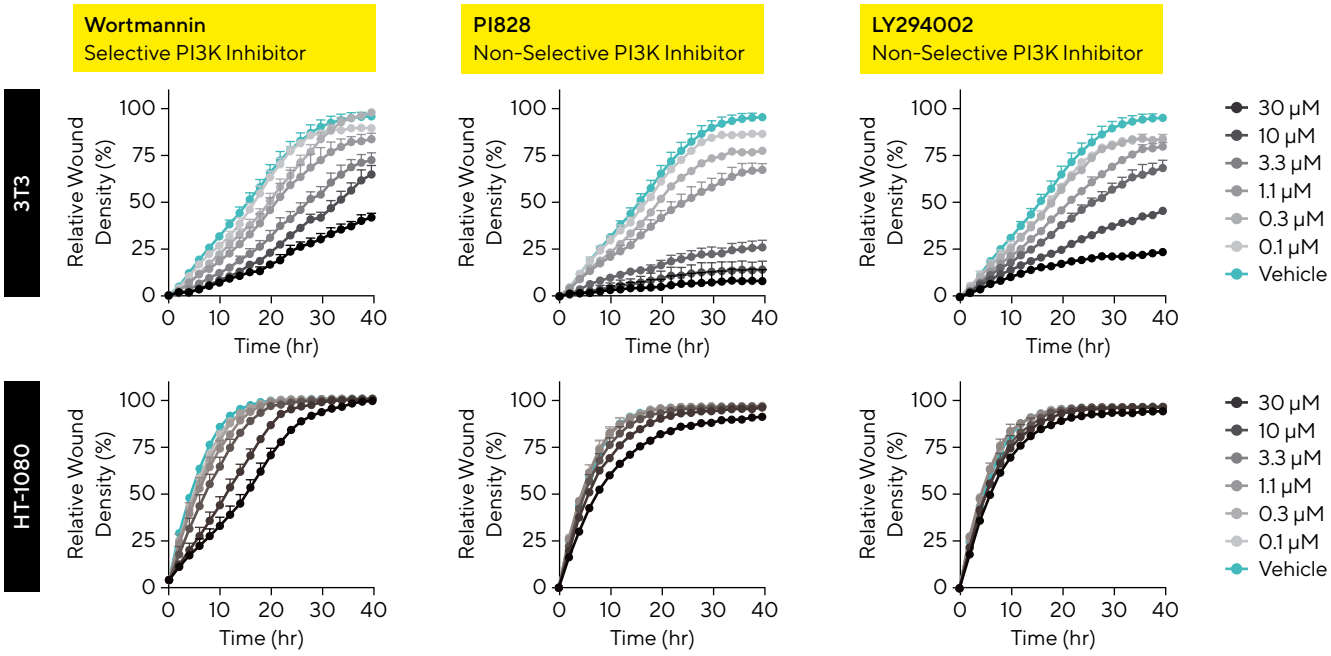

Figure 6: Cell-Type and Molecule-Dependent Temporal Cell Migration Profiles. 3T3 and HT-1080 cells (30,000 cells/well) were wounded and treated with a concentration range (0.1–30 µM) of PI3K inhibitors: Wortmannin, PI828, and LY294002. Data show varying kinetic migratory profiles in the presence of different compounds. PI3K inhibitors showed a significant difference in efficacy across cell types with HT-1080 cells appearing more resistant to PI3K inhibition compared to 3T3 cells. Data shown as mean ± SEM, n = 3 replicates.

Cell Cycle and Migration

Cell migration and proliferation play essential roles in both physiological and pathological events, such as tumor metastasis. We can gain insights into cell cycle progression via cells expressing the Incucyte® Cell Cycle Lentivirus Reagents. These cells express green fluorescence in S|G2|M phases of the cell cycle, red (or orange) fluorescence in G1, yellow fluorescence (red or orange + green) in transition phases G1→S, and non-fluorescence in M→G1 (Figure 7A). The Incucyte® Scratch Wound Analysis Software Module enables quantification of the two most prominent populations: green and red (or orange). To calculate populations within the wound, we determined the total count of red and green cells within the wound and expressed the red or green values as a percentage of the total count. Through utilizing these cells within a Scratch Wound Assay, both cell migration and cell cycle dynamics can be characterized simultaneously in real time.

HT-1080 cells expressing Incucyte® Cell Cycle Green/Red Lentivirus were wounded and treated with cytochalasin D. Fluorescence images reveal inhibition of cell migration and cell cycle arrest, where a high percentage of cells are in G1 and display red fluorescence for cytochalasin D compared to vehicle (Figure 7B). Time-courses confirm this, demonstrating that cytochalasin D has an inhibitory effect on migration (RWD) and arrests the cell cycle in G1 (% Red Population) (Figure 7C). This is consistent with previous data where cytochalasin D significantly affects actin polymerization, and thus migration, and activates p53-dependent pathways causing arrest at the G1-S transition.[11]

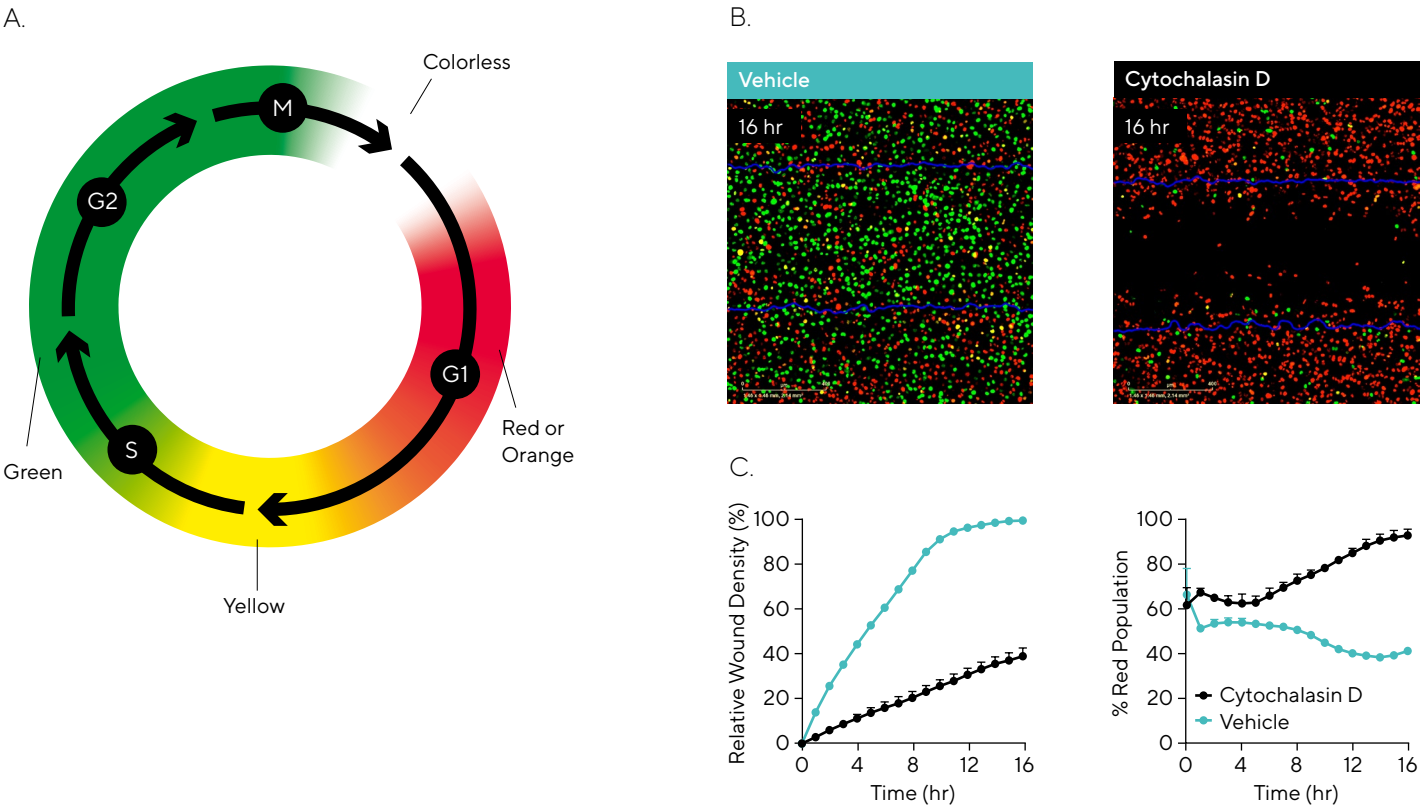

Figure 7: Concurrent Measurements of Cell Cycle Progression and Cell Migration. HT-1080 cells stably expressing the Incucyte® Cell Cycle Green/Red Lentivirus (30,000 cells/well) were wounded and then treated with 0.31 µM cytochalasin D. Phase and dual fluorescence metrics were used to quantify cell migration and cell cycle progression, respectively. (A) Schematic displays the fluorescence color expression of cells during the cell cycle. Utilizing the Incucyte® Scratch Wound Analysis Software Module we can quantify cells exhibiting red fluorescence in G1 and green fluorescence in S|G2|M. (B) Green and red fluorescence images reveal inhibition of cell migration (initial scratch outline in blue) and a high population in red, indicating cell cycle arrest in G1 for cytochalasin D compared to vehicle. (C) Time-courses indicate that cytochalasin D has an inhibitory effect on cell migration (Relative Wound Density) and the cell cycle through arresting in G1 (% Red Population). Data shown as mean ± SEM, n = 3 replicates.

To compare mechanistic compound effects, MDA-MB-231 cell cycle cells were treated with anti-migratory PP242 and anti-proliferative MMC. Time-courses revealed PP242 affects both cell migration and the cell cycle in a concentration-dependent manner, causing inhibition of wound closure and cell cycle arrest in the G1 (red) phase. Transformation of the data exhibits these concentration-dependent effects (IC_{50} of 1.69 µM and EC_{50} of 0.95 µM, respectively) (Figure 8A). Contrastingly, MMC had no effect on migration over 24 hours, yet did exhibit a kinetic concentration-dependent effect on the cell cycle by arresting in the S|G2|M (green) phase (IC_{50} of 1.25 µM) (Figure 8B). Images allow for visualization of compound effects on migration (initial scratch outline in blue) and cell cycle arrest (green or red fluorescence) compared to vehicle (Figure 8C).

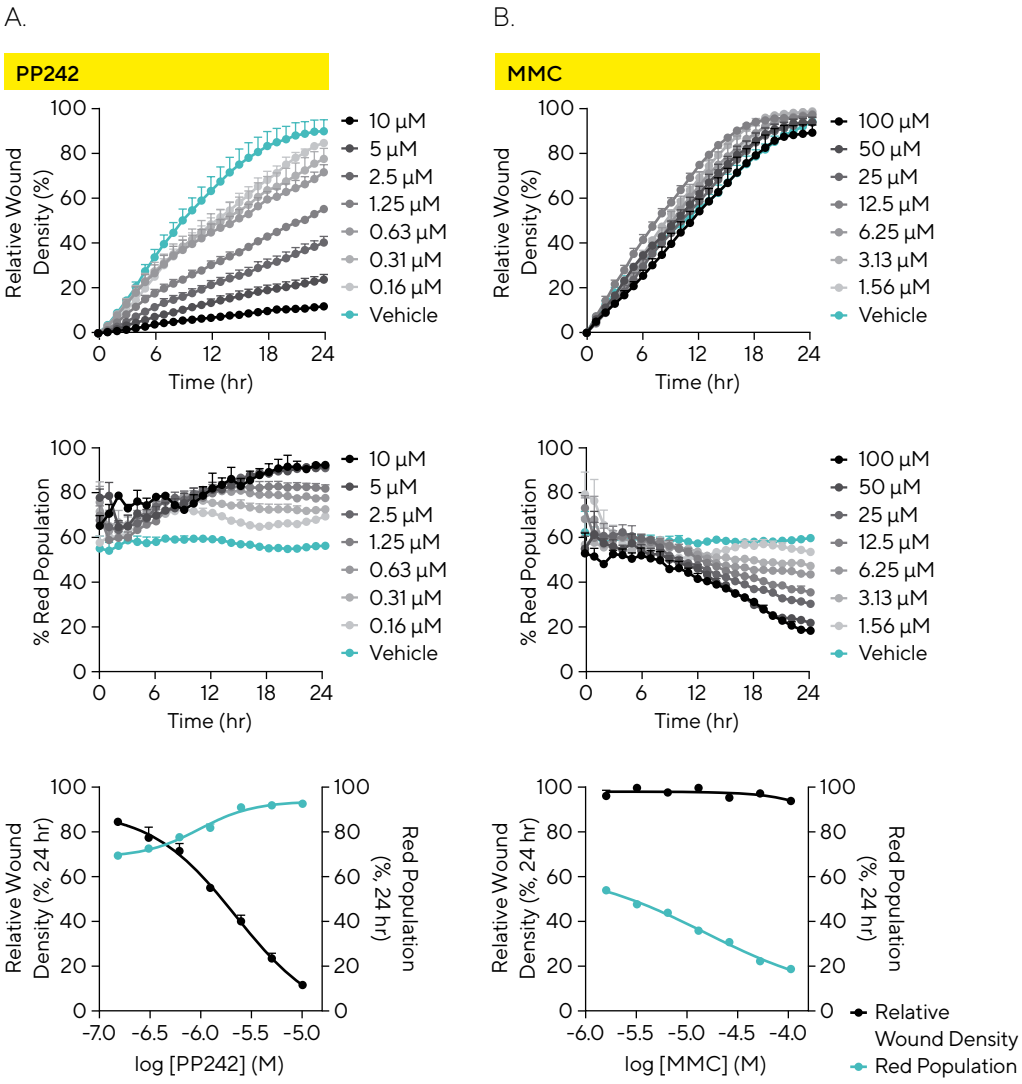

Figure 8: Differential Effects of Compounds on Cell Cycle and Cell Migration. MDA-MB-231 cells stably expressing Incucyte® Cell Cycle Green/Red Lentivirus (30,000 cells/well) were wounded and treated with PP242 or mitomycin C (MMC). Time-courses and concentration response curves indicate: (A) PP242 had a concentration-dependent effect on cell migration (relative wound density) and the cell cycle with an increase in the red cell population (G1) within the wound (red population); (B) In contrast MMC had no little-to-no effect on migration but had a concentration-dependent effect on the cell cycle with an arrest in green (S|G2|M) as shown by a decreasing red population; (C) Fluorescence images enable visualization of cell migration (initial scratch outline in blue) and cell cycle arrest for treated and vehicle conditions (24 hours post-scratch). Data shown as mean ± SEM, n = 3 replicates.

Summary and Outlook

In this application note, we highlight the use of the Incucyte® Scratch Wound Assay for flexible and robust quantification of cell migration. High quality images enable visualization of the morphology changes that accompany migration and accurate quantification using integrated software, which provides kinetic and pharmacological migration profiles. Dual fluorescence readouts give additional insight and enable measurements of cell cycle dynamics alongside cell migration. With the strong links to oncological research, it is clear why facilitating research into cell migration is imperative to furthering our understanding.

References

1. Gagliardi P, Puliafito A, di Blasio L, et al. Real-time monitoring of cell protrusion dynamics by impedance responses. *Scientific Reports*. 2015;5(1).
2. Kim D, Wirtz D. Focal adhesion size uniquely predicts cell migration. *The FASEB Journal*. 2012;27(4):1351-1361.
3. Alix-Panabieres C, Magliocco A, Cortes-Hernandez L, Eslami-S Z, Franklin D, Messina J. Detection of cancer metastasis: past, present and future. *Clinical & Experimental Metastasis*. 2021;39(1):21-28.
4. Yang J, Gong X, Ouyang L, He W, Xiao R, Tan L. PREX2 promotes the proliferation, invasion and migration of pancreatic cancer cells by modulating the PI3K signaling pathway. *Oncology Letters*. 2016;12(2):1139-1143.
5. Gad S. Mitomycin C. In: Wexler P, ed. *Encyclopedia of Toxicology (Third Edition)*. Academic Press; 2014:354-356.
6. Kumar V, Ali M, Ramachandran C. Effect of mitomycin-C on contraction and migration of human nasal mucosa fibroblasts: implications in dacryocystorhinostomy. *British Journal of Ophthalmology*. 2015;99(9):1295-1300.
7. Taniguchi M, Saito, K, Aida R, Ochiai A, Saitoh E, Tanaka T. Wound healing activity and mechanism of action of antimicrobial and lipopolysaccharide-neutralizing peptides from enzymatic hydrolysates of rice bran proteins. *Journal of Bioscience and Bioengineering*. 2019;128(2):142-148.
8. Biswas D, Hyun S. Supplementation of fetal bovine serum increased the quality of in vitro fertilized porcine embryo. Journal of Advanced Veterinary and Animal Research. 2021;8(4).
9. Fattahi S, Amjadi-Moheb F, Tabaripour R, Ashrafi G, Akhavan-Niaki H. PI3K/AKT/mTOR signaling in gastric cancer: Epigenetics and beyond. *Life Sciences*. 2020;262.
10. Gupta S, Stuffrein S, Plattner R, Tencati M, Gray C, Whang Y, Stanbridge E. Role of Phosphoinositide 3-Kinase in the Aggressive Tumor Growth of HT1080 Human Fibrosarcoma Cells. *Molecular and Cellular Biology*. 2001;21(17):5846-5856.
11. Trendowski M. Using Cytochalasins to Improve Current Chemotherapeutic Approaches. *Anti-Cancer Agents in Medicinal Chemistry*. 2015;15(3):327-335.

North America
Sartorius Corporation
300 West Morgan Road
Ann Arbor, Michigan 48108
USA
Phone +1 734 769 1600
Email: orders.US07@sartorius.com

Europe
Sartorius UK Ltd.
Longmead Business Centre
Blenheim Road
Epsom
Surrey, KT19 9QQ
United Kingdom
Phone +44 1763 227400
Email: euorders.UK03@sartorius.com

Asia Pacific
Sartorius Japan K.K.
4th Floor, Daiwa Shinagawa North Bldg.
1-8-11, Kita-Shinagawa 1-chome
Shinagawa-Ku
Tokyo 140-0001
Japan
Phone +81 3 6478 5202
Email: orders.US07@sartorius.com

Find out more: www.sartorius.com/incucyte

For questions, email: AskAScientist@sartorius.com